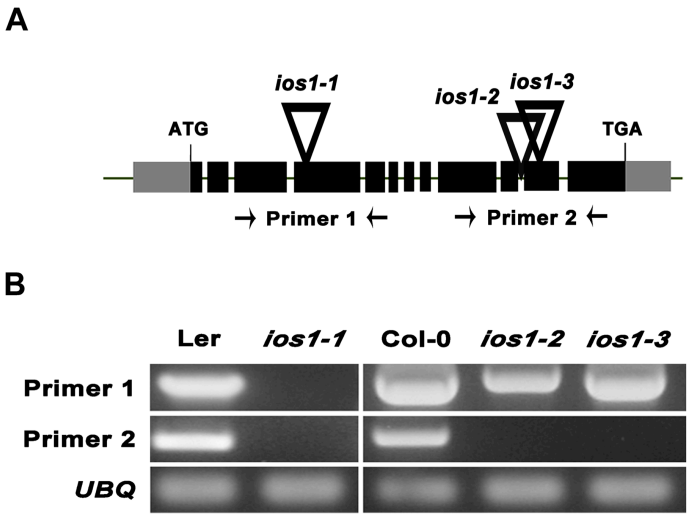

Supplemental Figure 1. The mutant *ios1-1* is a knock-out but *ios1-2* and *ios1-3* still produce some *IOS1* transcripts.

(**A**) Insertion sites in the *Ds* transposon insertion mutant *ios1-1*, and T-DNA insertion mutants *ios1-2* and *ios1-3*. Bold lines, exons; thin lines, introns; bold arrows, sites of insertion; thin arrows, primers used for RT-PCR.

(**B**) *IOS1* expression in L*er*-0 WT and *ios1-1* and Col-0 WT, *ios1-2* and *ios1-3*. Analyses were performed by RT-PCR for 30 cycles. *UBQ10* was used as a loading control.

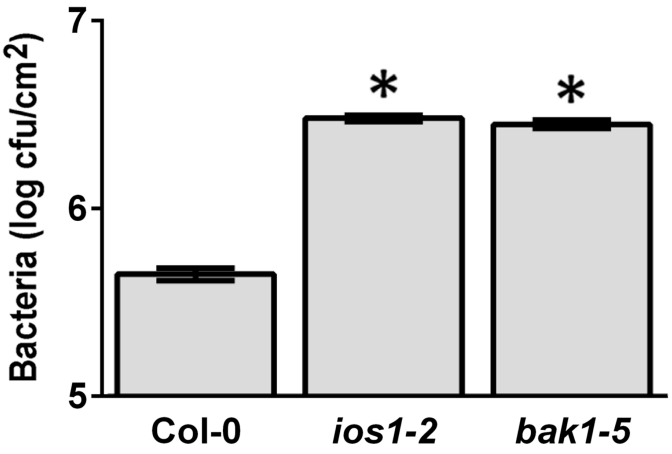

Figure 2. Susceptibility phenotypes of *ios1-2* and *bak1-5* to *Pst* DC3000.

Bacterial titers were evaluated at 2 dpi in 5-week-old Arabidopsis Col-0 WT, *ios1-2,* and *bak1-5* dip-inoculated with 10^6 cfu/mL *Pst* DC3000. Averages ± SE of 2 independent experiments each with 3 plants (n = 6). Asterisks indicate a significant difference to WT controls based on a paired two-tailed *t* test ($P < 0.01$).

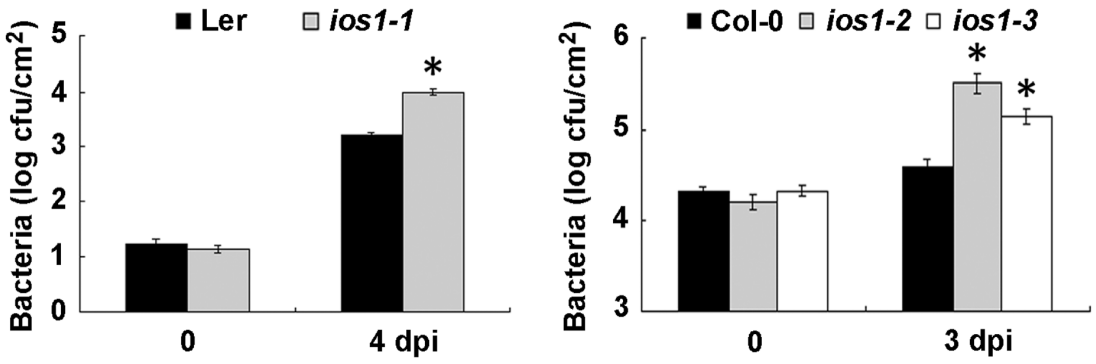

Figure 3. *ios1* mutants demonstrate increased susceptibility to *Pst* DC3000 *hrcC*$^-$.

Bacterial titers were evaluated in 5-week-old Arabidopsis syringe-infiltrated with 10^5 cfu/mL *Pst* DC3000 *hrcC*$^-$ for L*er*-0 and *ios1-1*, and 10^8 cfu/mL *Pst* DC3000 *hrcC*$^-$ for Col-0, *ios1-2* and *ios1-3*. Data ± SE represent average of 3 independent experiments each consisting of 3 plants (n = 9). Asterisks indicate a significant difference to respective WT controls based on a paired two-tailed *t* test ($P < 0.01$). dpi = days post inoculation.

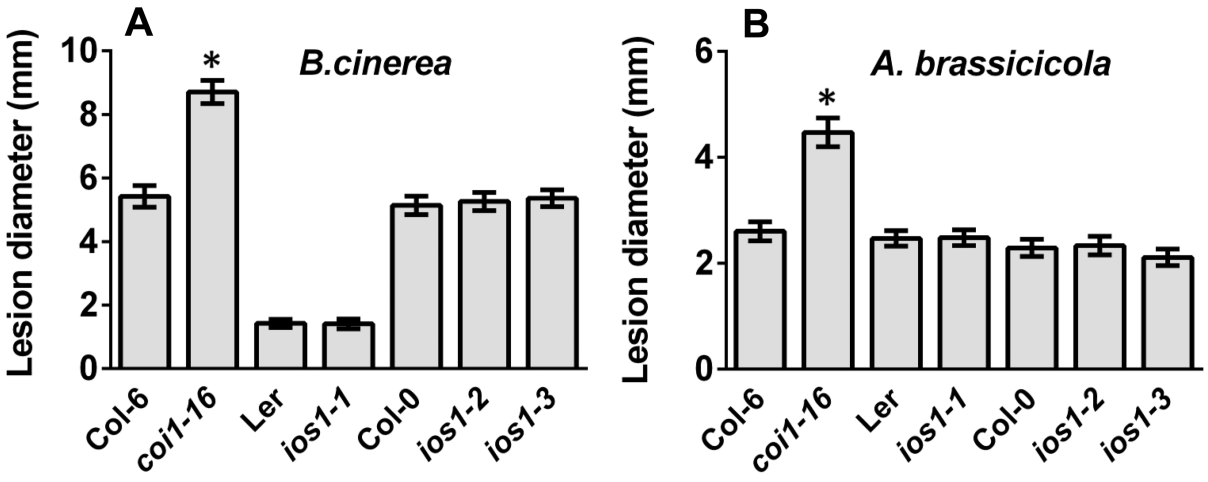

Figure 4. Resistance of *ios1* mutants to necrotrophic fungal pathogens.

(**A**) *B. cinerea*-mediated necrosis. Arabidopsis L*er*-0 and Col-0 WT and corresponding *ios1-1*, *ios1-2,* and *ios1-3* mutants leaves were droplet-inoculated (10 µL) with 10^5 *B. cinerea* spores/mL and lesion diameters were evaluated at 3 dpi. Data ± SD represent 2 independent experiments each consisting of 6 plants (n = 12). Asterisks indicate a significant difference to respective WT controls based on a paired two-tailed *t* test ($P < 0.05$). The mutant *coi1-16* (Col-6 background) is known to be highly susceptible to *B. cinerea* and was thus used as a positive control.

(**B**) *A. brassicicola*-mediated necrosis. Arabidopsis L*er*-0 and Col-0 WT and corresponding *ios1-1*, *ios1-2,* and *ios1-3* mutants leaves were droplet-inoculated (10 µL) with 5 x 10^5 *A. brassicicola* spores/mL and lesion diameters were evaluated at 4 dpi. Data ± SD represent 2 independent experiments each consisting of 6 plants (n = 12). Asterisks indicate a significant difference to respective WT controls based on a paired two-tailed *t* test ($P < 0.05$). The mutant *coi1-16* (Col-6 background) is known to be hyper-susceptible to *A. brassicicola* and was thus used as a positive control.

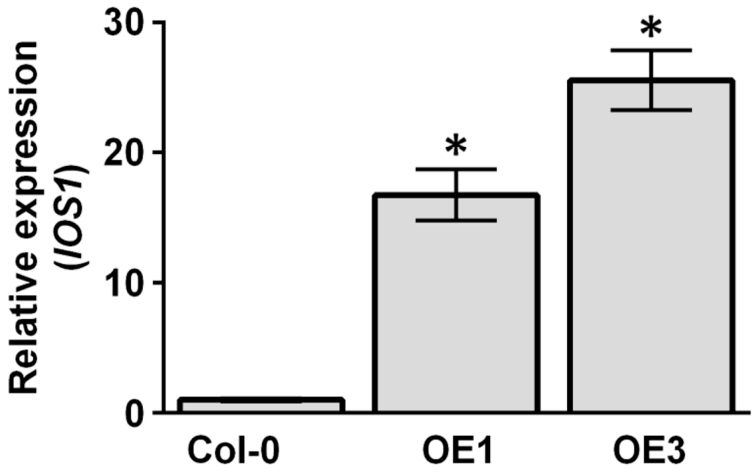

Figure 5. *IOS1* mRNA expression levels in 2 independent *IOS1* over-expression lines.

Gene expression levels in 10-day-old seedlings of 2 lines over-expressing *IOS1* (OE1 and OE3) relative to Col-0 WT (defined value of 1) were analyzed by RT-qPCR. *UBQ10* was used for normalization. Results are means ± SD of 2 independent experiments with 3 plants each (n = 6). Asterisks indicate a significant difference to WT controls based on a paired two-tailed *t* test ($P < 0.01$).

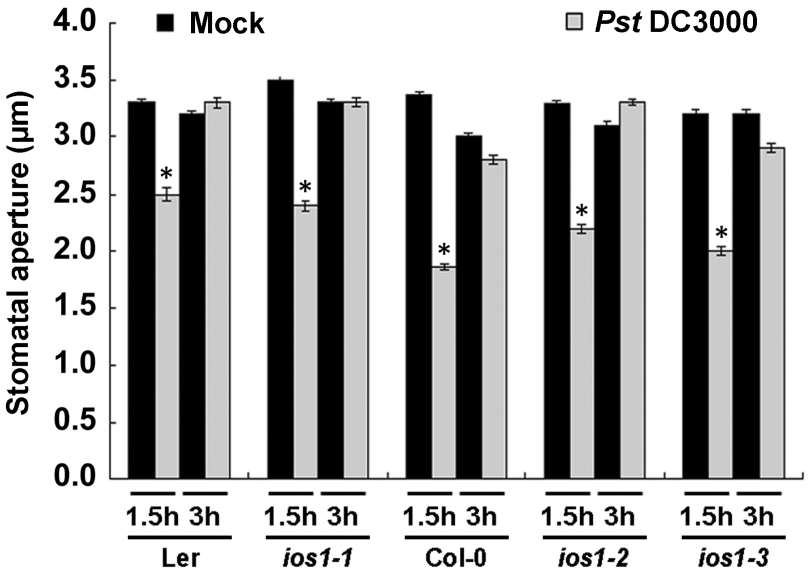

Figure 6. Stomatal innate immunity in *ios1* mutants.

Stomatal apertures in epidermal peels were analyzed after 1.5 h and 3 h exposure to $MgSO_4$ (Mock) or 10^8 cfu/mL *Pst* DC3000 in L*er*-0 and *ios1-1* and Col-0, *ios1-2* and *ios1-3*. Results are shown as mean ± SE of 3 independent experiments each consisting of at least 60 stomata (n > 180). Asterisks indicate a significant difference to mock control based on a paired two-tailed *t* test analysis ($P < 0.001$).

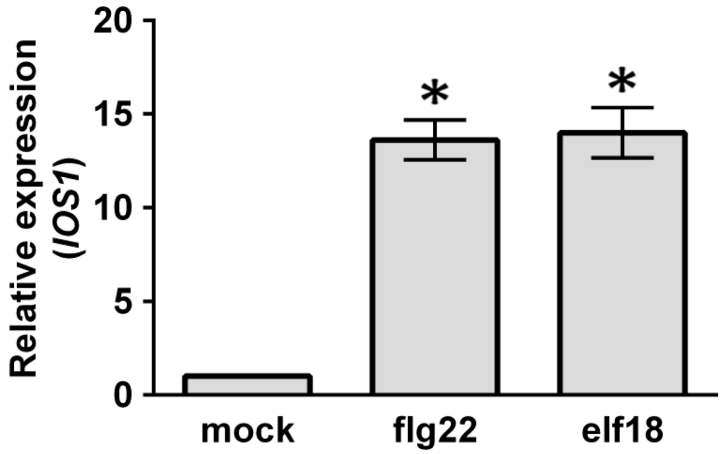

Figure 7. Expression of *IOS1* is up-regulated by bacterial MAMPs.

IOS1 relative expression levels in 10-day-old seedlings at 1 h after treatment with 100 nM flg22 or elf18 were determined by qRT-PCR analysis. *UBQ10* was used for normalization. Relative expression levels were compared to mock, buffer-treated control (defined value of 1). Values are means ± SD of 2 independent experiments with 3 plants each (n = 6). Asterisks indicate a significant difference to mock control based on a paired two-tailed *t* test ($P < 0.01$).

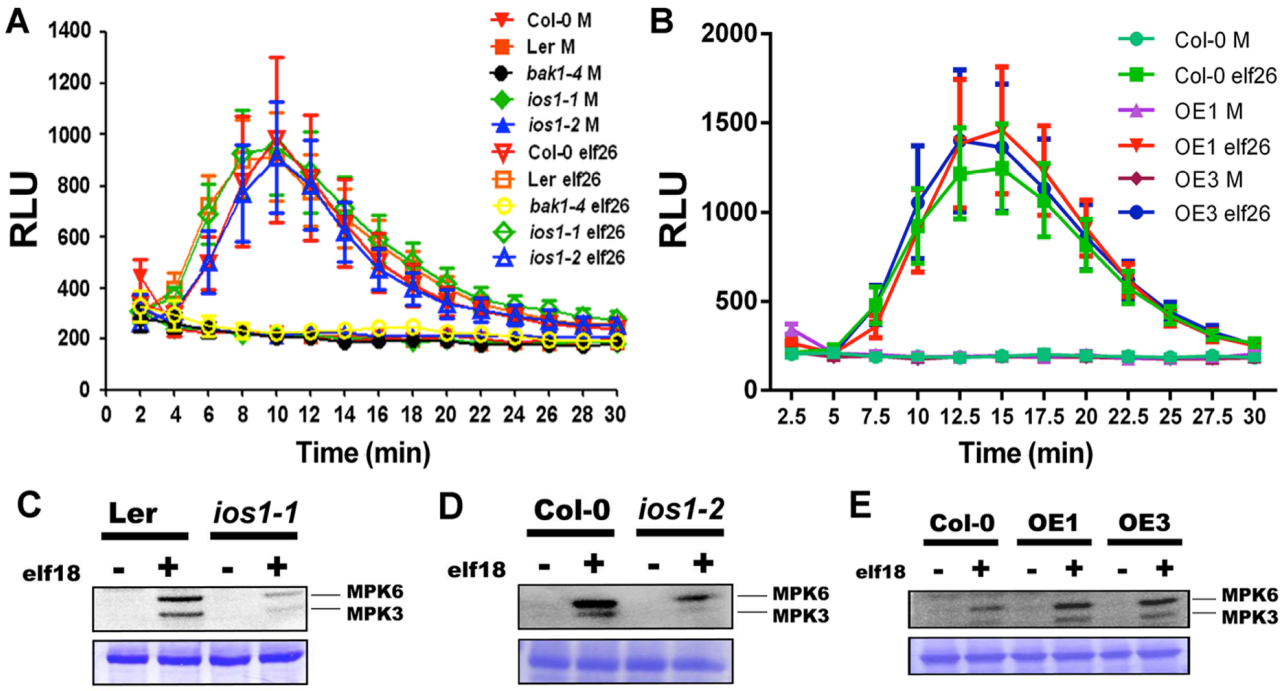

Figure 8. Early PTI responses.

(**A**) ROS production in *ios1* mutants. Responsiveness of 5-week-old L*er*-0 and Col-0 WT controls and respective mutants *ios1-1* and *ios1-2* to 10 nM elf26. *bak1-4* was used as a negative control. Production of ROS in Arabidopsis leaf discs is expressed as relative light units (RLU) for a period of 30 min after elicitation. Values are means ± SE of 3 independent experiments each with 6 leaf discs (n = 18). Differences between *ios1* mutants and WT were not statistically significant based on a paired two-tailed *t* test ($P < 0.01$).

(**B**) ROS production in *IOS1*-OE lines. Responsiveness of 5-week-old over-expression lines OE1 and OE3 and Col-0 WT control to 10 nM elf26. Production of ROS in Arabidopsis leaf discs is expressed as relative light units (RLU) for a period of 30 min after elicitation. Values are means ± SE of 3 independent experiments each with 6 leaf discs (n = 18). Differences between OE lines and WT were not statistically significant based on a paired two-tailed *t* test ($P < 0.01$).

(**C and D**) MPK activation in *ios1* mutants. Ten-day-old L*er*-0 and *ios1-1* or Col-0 and *ios1-2* were treated with 100 nM elf18 for 5 min. Immunoblot analysis using phospho-p44/42 MPK antibody is shown in top panel. Lines indicate the positions of MPK3 and MPK6. Coomassie

Brilliant Blue-staining is used to estimate equal loading in each lane (bottom panel). Experiments were repeated twice with similar results.

(**E**) MPK activation in *IOS1*-OE lines. Ten-day-old Col-0 and *IOS1* over-expression lines OE1 and OE3 were syringe-infiltrated with 50 nM elf18 for 5 min. Immunoblot analysis using phospho-p44/42 MKP antibody is shown in top panel. Lines indicate the positions of MPK3 and MPK6. Coomassie Brilliant Blue-staining is used to estimate equal loading in each lane (bottom panel). Similar results were observed in another independent repeat.

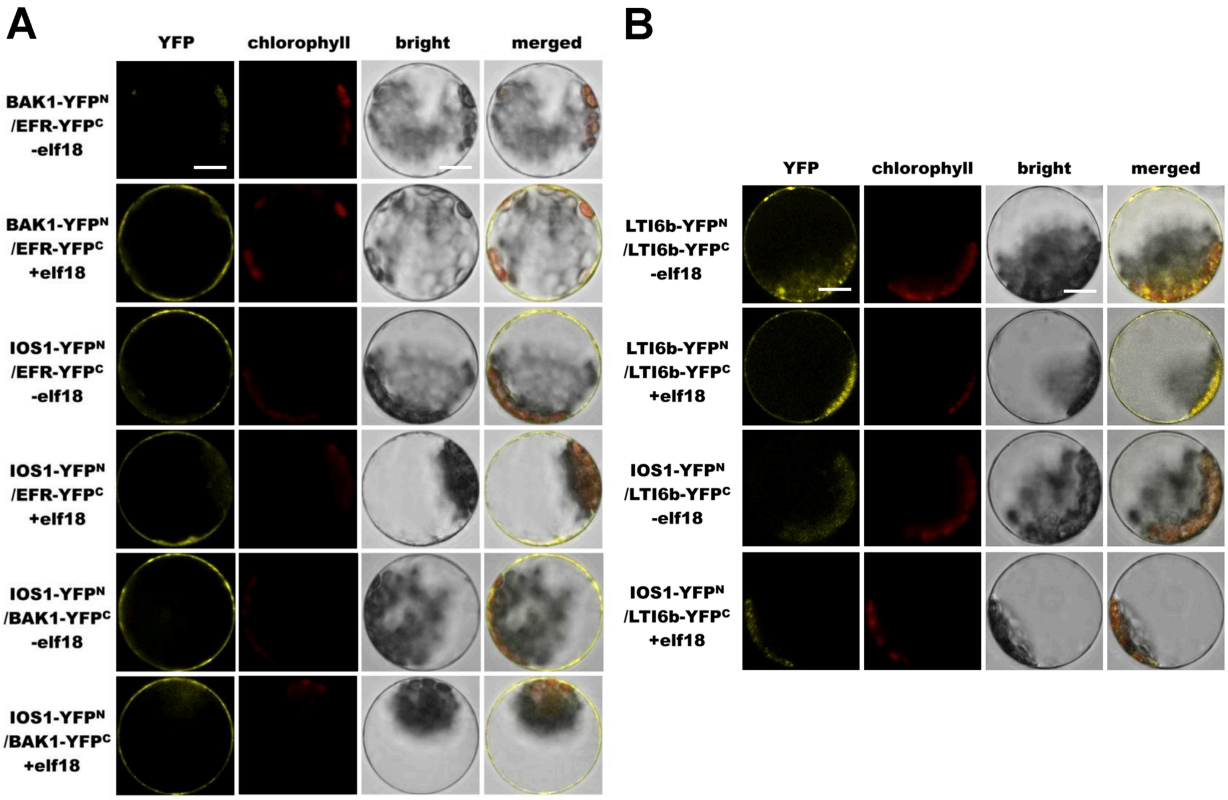

Figure 9. Bimolecular fluorescence complementation analyses of IOS1 interactions with EFR and BAK1.

(**A and B**) Arabidopsis protoplasts were co-transfected with BAK1-YFP^N + EFR-YFP^C, IOS1-YFP^N + EFR-YFP^C and IOS1-YFP^N + BAK1-YFP^C (A), LTI6b-YFP^N + LTI6b-YFP^C or IOS1-YFP^N + LTI6B-YFP^C (B) and treated with (+) or without (-) 100 nM elf18 for 10 min. The YFP fluorescence (yellow), chlorophyll autofluorescence (red), bright field and the combined images were visualized under a confocal microscope 16 h after transfection. Images are representative of multiple protoplasts. The experiment was repeated twice with similar results. Scale bars represent 10 μm.

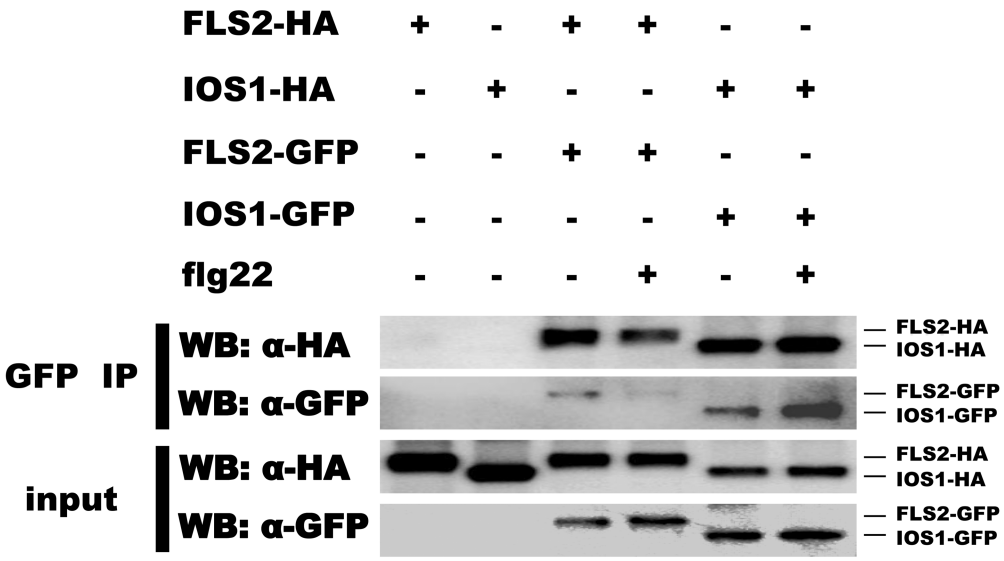

Figure 10. FLS2-FLS2 and IOS1-IOS1 dimerization.

Co-immunoprecipitation of FLS2-GFP and FLS2-HA_3 or IOS1-GFP and IOS1-HA_3 were performed by expression of FLS2-HA_3 or IOS1-HA_3 constructs only as a negative control or FLS2-GFP with FLS2-HA_3 or IOS1-GFP with IOS1-HA_3 in Arabidopsis protoplasts. Total proteins (input) were subjected to immunoprecipitation with GFP-Trap beads followed by immunoblot analysis with anti-HA antibodies to detect FLS2-HA_3 or IOS1-HA_3. Anti-GFP antibodies detect FLS2-GFP and IOS1-GFP. Experiments were repeated twice with similar results.

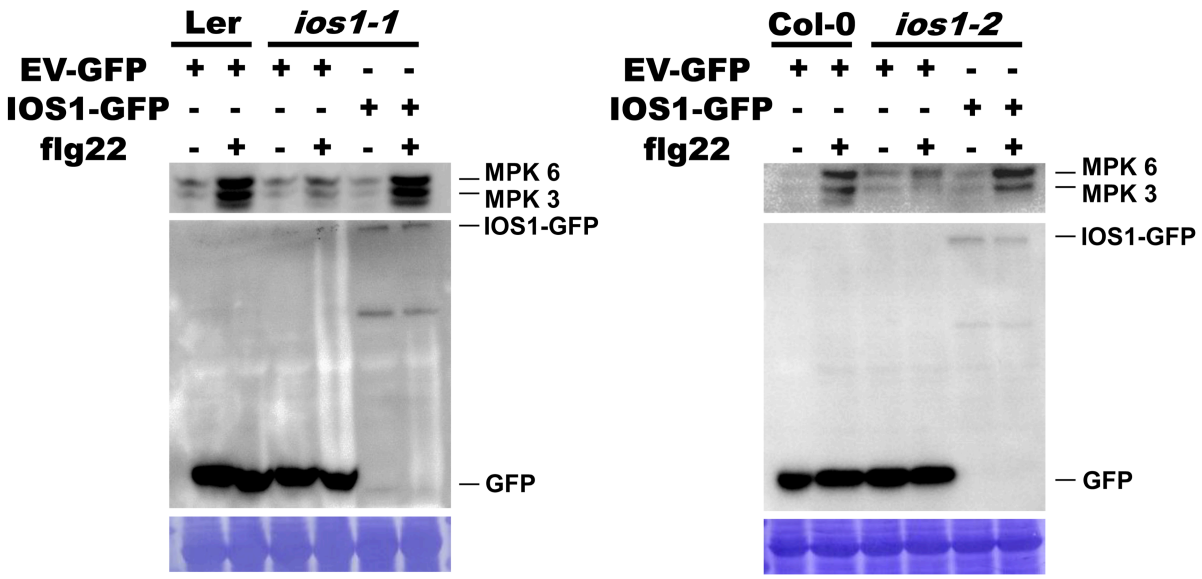

Figure 11. Complementation of defective MPK activation in *ios1-1* and *ios1-2* mutants by IOS1-GFP.

L*er*-0 and *ios1-1* or Col-0 and *ios1-2* Arabidopsis protoplasts expressing IOS1-GFP or the Empty Vector (EV)-GFP were treated with (+) or without (-) 100 nM flg22 for 5 min. Immunoblot analysis using phospho-p44/42 MPK antibody is shown in top panel. Lines indicate the positions of MPK3 and MPK6. Anti-GFP antibody detects IOS1-GFP and EV-GFP (middle panel). Coomassie Brilliant Blue-staining is used to estimate equal loading in each lane (bottom panel). Experiments were repeated twice with similar results.

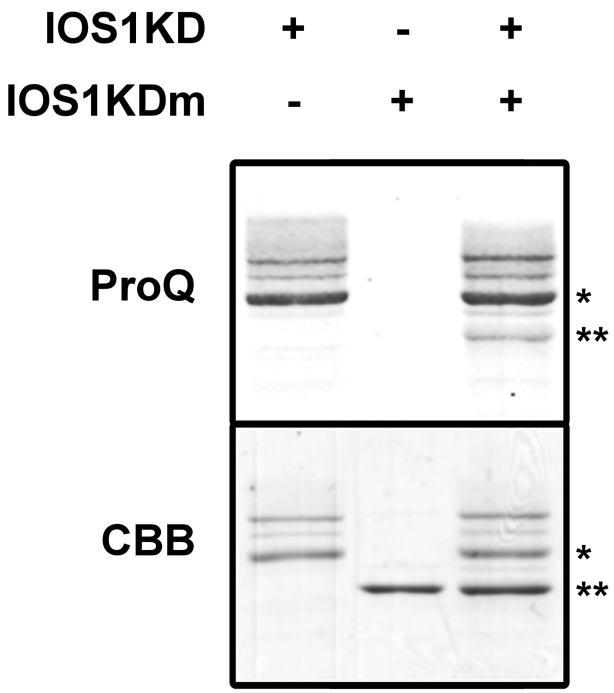

Figure 12. IOS1 *in vitro* autophosphorylation.

Two microgram of each affinity purified IOS1 active kinase (IOS1KD) and IOS1 kinase dead (IOS1KDm) were subjected to *in vitro* autophosphorylation reaction. SDS page of the whole reaction was stained by Pro-Q Diamond (ProQ), and subsequently stained with Coomassie Brillant Blue (CBB). One or two asterisks indicate the LC-MS/MS confirmed peptides for IOS1KD or IOS1KDm, respectively.

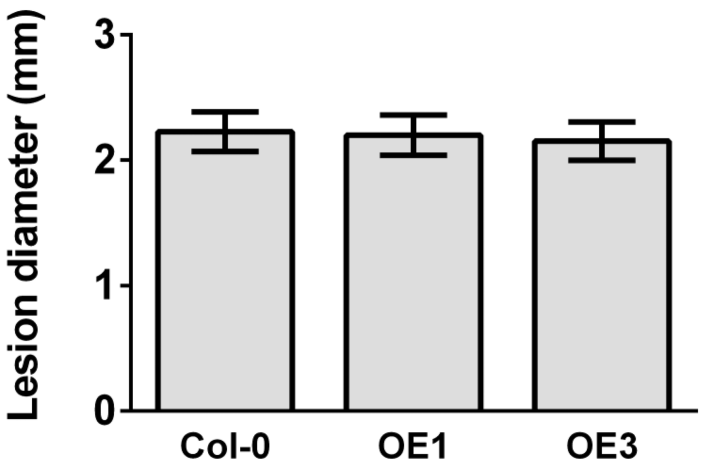

Figure 13. *A. brassicicola*-mediated lesions in lines overexpressing IOS1.

Arabidopsis leaves of Col-0 and *IOS1* overexpression lines OE1 and OE3 were droplet-inoculated (10 µL) with 5 x 10^5 *A. brassicicola* spores/mL and lesion diameters were evaluated at 4 dpi. Data are average ± SD of lesion diameters from 2 independent experiments each with 6 plants (n = 12). No significant differences to WT controls were observed when based on a paired two-tailed *t* test ($P < 0.01$).

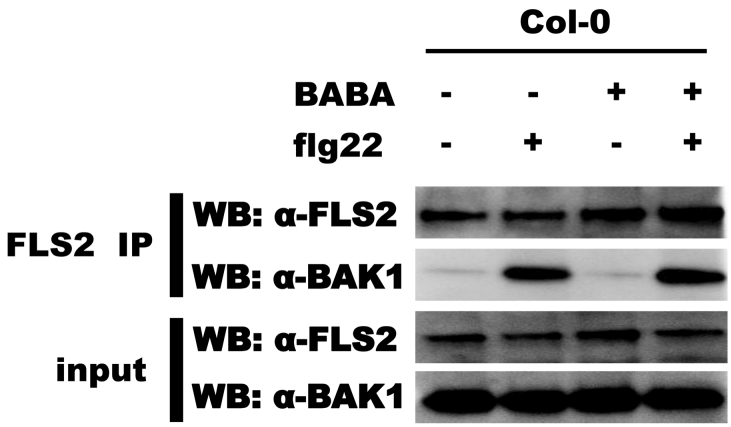

Figure 14. BABA does not regulate ligand-induced FLS2-BAK1 association.

Co-immunoprecipitation analysis was performed with seedlings grown on ½ MS plates with or without 30 μM BABA for 10 days and seedlings on the plates were submerged in a 100 nM flg22 solution for 10 min before collection. Total proteins (input) were subjected to immunoprecipitation (IP) with anti-FLS2 antibodies and IgG beads followed by immunoblot analysis using anti-FLS2 and anti-BAK1 antibodies. The experiment shown is one of 2 independent replicates.

Table 1. Identification of IOS1 tryptic peptides by HPLC-ESI-MS/MS analysis of EFR immunoprecipitates.

Peptide Sequence	Peptide probability	*n* Peptides	Occurrence[a]		Best Mascot Score
			no treatment	elf18 treatment	
(R)ADVGATVNQGYR(Y)	95%	6	3/8	2/8	71.44
(K)LADFGLSR(S)	95%	1	0/8	1/8	42.17
(K)TGNATPFISALELR(K)	95%	2	0/8	1/8	39.09
(R)TQFQQQTWNLR(S)	95%	8	2/8	3/8	62.96
(K)AEVELLLR(V)	95%	1	0/8	1/8	37.88
(K)RGPSILTWEGR(L)	95%	1	0/8	1/8	36.15
(R)YGIDVFDR(V)	95%	1	0/8	1/8	41.27
(R)KLTYIDVVK(I)	95%	3	2/8	1/8	37.82

[a]Occurrence of specific tryptic peptides in eight independent biological replicates combining 4 experiments performed using GFP-Trap beads and 4 experiments using anti-GFP magnetic beads for immunoprecipitation of EFR-GFP.

Table 2. Primer sequences used in this study.

Gene name	Purpose	Primer	Sequence
UBQ10 (At4g05320)	RT-qPCR/RT-PCR	Forward	5`- GGCCTTGTATAATCCCTGATGA -3'
		Reverse	5'- AAAGAGATAACAGGAACGGAAA -3'
FRK1 (At2g19190)	RT-qPCR	Forward	5'- GCCAACGGAGACATTAGAG -3'
		Reverse	5'- CCATAACGACCTGACTCATC -3'
IOS1 (At1g51800)	RT-qPCR	Forward	5'- CTTGACCGGAGAGATCTTAG -3'
		Reverse	5'- AGCTAGAGAAACTCTGGGACTG -3'
IOS1 CDS (At1g51800)	Plasmid constructs	Forward	5'- GCGCTACCACGAAAAAGAAG -3'
		Reverse	5'- CGCTTCCCTGATAAGTGCTC -3'
CERK1 CDS (At3g21630)	Plasmid constructs	Forward	5'-ATGAAGCTAAAGATTTCTCTAATCGCTC-3'
		Reverse	5'-CCGGCCGGACATAAGACTGACT-3'
IOS1 (At1g51800)	Primer 1, T-DNA RT-PCR	Forward	5'- CTTAATTTCACCACGTCTTCCG -3'
		Reverse	5'- GAGCAGAGGAGGTAAAGTCGAA -3'
IOS1 (At1g51800)	Primer 2, T-DNA RT-PCR	Forward	5'- GAAGCGTGGACCGTCGATACTA -3'
		Reverse	5'- GCAAACCGCAAATAGTTCACC -3'
ios1-1	Mutant line confirmation	Forward	5'- CAACCACGAACGAGACCGAAG -3'
		Reverse	5`- GCCGTAAGCCGACTTGATGTTC -3'
ios1-2	Mutant line confirmation	Forward	5'- TCCGTGAAGAAGACGGATTC -3'
		Reverse	5'- TAGCGAAAAACCGGAAATTG -3'
ios1-3	Mutant line confirmation	Forward	5'- TGCGGTAAAGATGCTCACACTG -3'
		Reverse	5'- TCATGTCTATCACGGGTTGG -3'
IOS1 (At1g51800)	Cytosolic domain cloning	Forward	5'- GGATCCAAGAGGAAGAAGAGAACC -3'
		Reverse	5'- CTCGAGTCATCTAGCTCCTGGATTAAGC -3'
IOS1 (At1g51800)	Site-directed mutagenesis	Forward	5'- GCAAATAGTTCACCGCAACATTAAGACTA CTAACATC -3'
		Reverse	5'- GATGTTAGTAGTCTTAATGTTGCGGTGAAC TATTTGC -3'